Molecular Therapy
Oncolytics
Original Article

The antitumor capacity of mesothelin-CAR-T cells in targeting solid tumors in mice

Qian Zhang,[1,7] Guoping Liu,[2,7] Jibin Liu,[3,7] Mu Yang,[4,7] Juan Fu,[5] Guodi Liu,[1] Dehua Li,[1] Zhangjie Gu,[1] Linsong Zhang,[1] Yingjiao Pan,[1] Xingbing Cui,[1] Lu Wang,[1] Lixin Zhang,[6] and Xiaoli Tian[1]

[1]Shanghai Yihao Biological Technology, Co., Ltd., Shanghai 200231, China; [2]Department of General Surgery, Changhai Hospital, Shanghai 200433, China; [3]Institute of Tumor of Nantong Tumor Hospital, No. 30, North Tongyang Road, Pingchao Town, Tongzhou District, Nantong City, Jiangsu Province 226361, China; [4]Department of Pathology, Shanghai General Hospital, Shanghai Jiaotong University School of Medicine, Shanghai 200080, China; [5]Department of Obstetrics and Gynecology, the First Affiliated Hospital of Dalian Medical University, Dalian 116000, China; [6]State Key Laboratory of Bioreactor Engineering, East China University of Science and Technology, Room 18-201, 130 Meilong Road, Shanghai 200237, China

Since the approval of chimeric antigen receptor (CAR) T cell therapy targeting CD19 by the FDA, CAR-T cell therapy has received increasing attention as a new method for targeting tumors. Although CAR-T cell therapy has a good effect against hematological malignancies, it has been less effective against solid tumors. In the present study, we selected mesothelin (MSLN/MESO) as a target for CAR-T cells because it is highly expressed by solid tumors but only expressed at low levels by normal tissues. We engineered a third generation MSLN-CAR comprising a single-chain variable fragment (scFv) targeting MSLN (MSLN-scFv), a CD8 transmembrane domain, the costimulatory domains from CD28 and 4-1BB, and the activating domain CD3ζ. *In vitro*, MSLN-CAR-T cells killed various solid tumor cell lines, demonstrating that it could specifically kill MSLN-positive cells and release cytokines. *In vivo*, we investigated the effects of MSLN-CAR-T cell therapy against ovarian, breast, and colorectal cancer cell-line-derived xenografts (CDX) and MSLN-positive colorectal and gastric cancer patient-derived xenografts (PDX). MSLN-CAR decreased the growth of MSLN-positive tumors concomitant with significantly increased T cells and cytokine levels compared to the control group. These results indicated that modified MSLN-CAR-T cells could be a promising therapeutic approach for solid tumors.

INTRODUCTION

Malignant tumors seriously endanger human health and life. The Global Cancer Statistics 2018 estimated that there would be 18.1 million new cancer cases (17.0 million excluding nonmelanoma skin cancer) and 9.6 million cancer deaths (9.5 million excluding nonmelanoma skin cancer) in 2018.[1] The top ten most common cancers are solid tumors. For both sexes combined, lung cancer is the most commonly diagnosed cancer (11.6% of total cases) and the leading cause of cancer death (18.4% of the total cancer deaths), closely followed by female breast cancer (11.6%), colorectal cancer (10.2%), and prostate cancer (7.1%) for incidence and colorectal cancer (9.2%), stomach cancer (8.2%), and liver cancer (8.2%) for mortality.[2] At present, the treatment of solid tumors is still mainly based on surgical resection, radiotherapy and chemotherapy, and targeted therapy; however, these methods often fail to eradicate tumor lesions, leading to tumor recurrence and progression.

Immunotherapy is a promising treatment option for hematological and solid tumors.[3] Chimeric antigen receptor (CAR) T cells are genetically engineered T cells, characterized by their tumor-specific, major histocompatibility complex-independent, and immune-mediated cytolytic actions.[4] In 2017, two CAR-T cell therapies against acute lymphoblastic leukemia (ALL) and advanced lymphomas were approved by the US Food and Drug Administration (FDA). Therefore, CAR-T cell therapy might represent a potential cure for cancer patients. However, compared to hematological cancers, the response rates of CAR-T cell therapy against solid cancers have been less successful. Currently, there is an increased effort to modulate the immunosuppressive tumor microenvironment and enhance the CAR-T cell antitumor effects in solid cancers.[5]

The CAR is a fusion protein consisting of three components: an extracellular antigen recognition domain, which is a single-chain variable fragment (scFv) that recognizes the tumor-associated antigen (TAA); intracellular signaling domains (e.g., OX40, CD28, and 4-1BB [CD137]) involved in the activation and the killing effect of T cells; and a CD3ζ T cell activating domain. These components help target and wipe out tumor cells.[6] Mesothelin (MSLN) is a 40-kDa membrane protein attached to the cell surface by phosphatidylinositol and is reportedly expressed by solid tumors.[7–10] A recent study used MSLN to target various solid cancers;[9–11] however, the use of modified MSLN-CAR-T cells to treat solid tumors requires further investigation.

Received 21 October 2020; accepted 18 February 2021;
https://doi.org/10.1016/j.omto.2021.02.013.

[7]These authors contributed equally

Correspondence: Lixin Zhang, State Key Laboratory of Bioreactor Engineering,East China University of Science and Technology, Room 18-201, 130 Meilong Road, Shanghai 200237, China.
E-mail: lxzhang@ecust.edu.cn
Correspondence: Xiaoli Tian, Shanghai Yihao Biological Technology, Co., Ltd., Shanghai 200231, China.
E-mail: ceo@shmlrs.cn

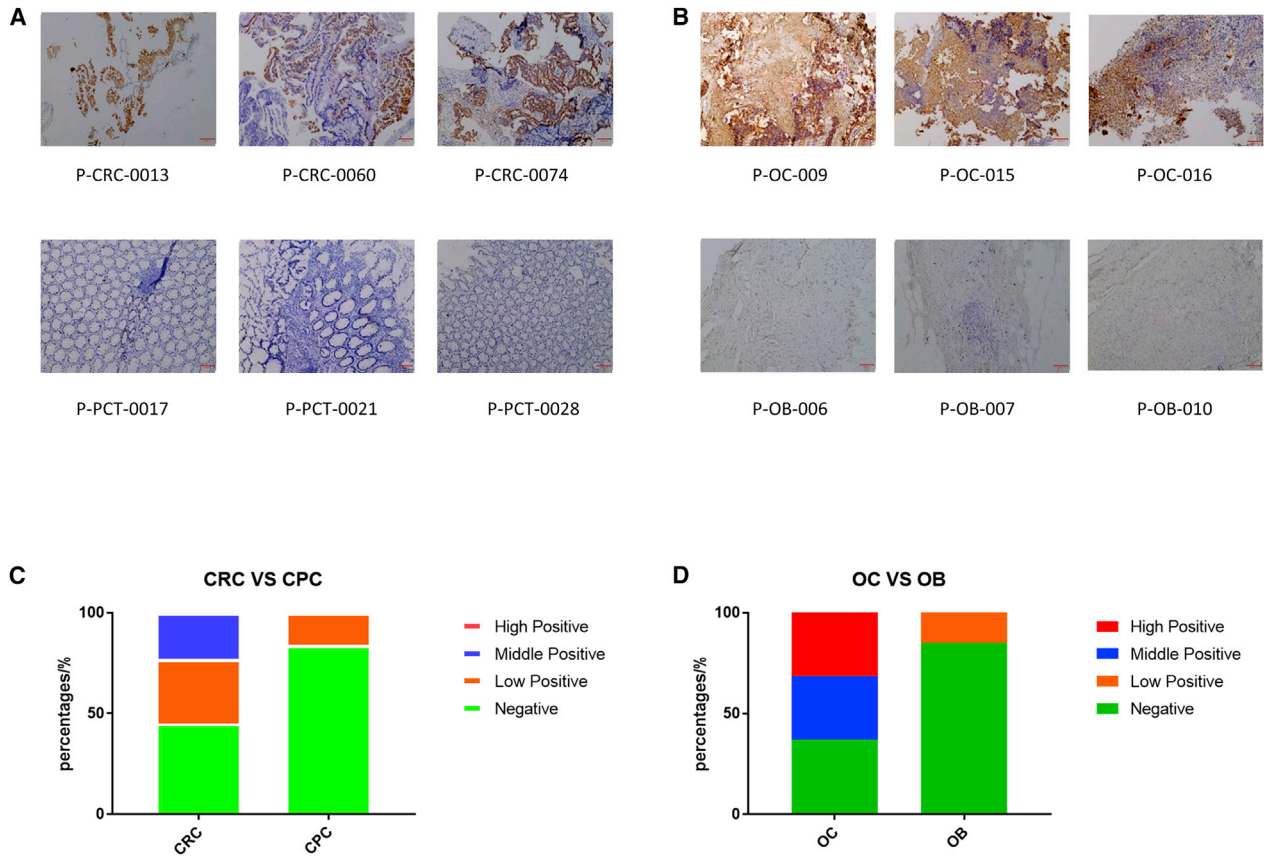

Figure 1. High expression of MSLN in CRC and OC samples

(A and B) MSLN expression was detected in CRC, CPC, OC, and OB tissues. CRC, colorectal cancer; CPC, colorectal para-cancerous tissue; OC, ovarian cancer tissue sample; OB, ovarian benign tissue. Scale bar, 100 μm. (C and D) Comparison of MSLN expression level between CRC and CPC or OC and OB groups. Stacked bar graph was derived from the Tables 1 and 2. High positive means positive target expression >50%, medium positive means positive target expression 20%~50%, and low positive means positive target expression <20%.

Patient-derived xenograft (PDX) models have been widely used in translational cancer research because they faithfully resemble the original tumors and maintain this similarity across passages.[12–15] In this study, we generated gastric and intestinal cancer PDX models with strong MSLN expression and cell line-derived xenograft (CDX) models of different cancer types that express MSLN. We found that MSLN-CAR-T cells had a good anti-tumor effect against all of the tumor models. Our study indicated that MSLN-CAR-T cells could represent a new therapy for patients with solid tumors.

RESULTS

High MSLN expression in ovarian and colorectal cancer

MSLN levels were measured in 72 cancer tissues (19 ovarian, 53 colorectal) and 38 non-cancerous tissues (13 ovarian benign [OB] tissue, 25 colorectal para-cancerous [CPC] tissue) by immunohistochemistry (IHC). Although MSLN was expressed in both cancerous and non-cancerous tissue, there was a large difference in expression levels between the two groups (Figures 1A and 1B). Among the 53 colorectal cancer and 25 adjacent tissue samples, we identified three groups of MSLN-positive samples: high (>50%), medium (20% to 50%), and low (<20%). There was a MSLN expression rate of 55% for the colorectal cancer samples, while the rate of the adjacent tissue samples was only 16% (Table 1; Figure 1C). Similarly, we found a 63% MSLN expression rate for the 19 ovarian cancer samples, but MSLN was only expressed in 15% of the 13 non-cancerous normal ovaries (Table 2; Figure 1D). The MSLN expression levels in all the positive ovarian cancer samples were above the medium level. According to the experimental results, a significantly higher expression of MSLN was found in ovarian and colorectal cancer tissue samples, while negative and lower expression levels were observed in normal ovarian and colorectal tissue samples. Although we only evaluated MSLN expression in intestinal and ovarian cancer and non-cancerous tissue, our results were comparable to those reported previously.[16] Together, these data indicate that because of the high expression

Table 1. MSLN positivity rate in CRC and CPC samples

	Totals	High positive	Medium positive	Low positive	Negative	Positive rate (%)
CRC	53	0	12	17	24	54.7
CPC	25	0	0	4	21	16

CRC, colorectal cancer tissue; CPC, colorectal para-cancerous tissue

of MSLN in solid tumors compared to normal or adjacent tissue, MSLN could be an important therapeutic target for ovarian and colorectal cancer. Its tumor specificity would increase the safety of this approach.

Construction of third generation MSLN-CAR-T cells targeting MSLN

To treat solid tumors, we designed a third generation CAR-T-targeting MSLN: the TAA on the cancer cell surface. We engineered a lentiviral vector to express a scFv of antibody that recognized MSLN (MSLN-scFv), a CD8 transmembrane domain, the costimulatory domains from both CD28 and 4-1BB, and the T cell activating domain CD3ζ to generate MSLN-CAR (Figure 2A). The surface expression of MSLN-CAR on activated T cells was determined by flow cytometry using biotinylated human MSLN. We found that 38% of the infected T cells were MSLN-CAR-positive (MSLN-CAR-T cells; Figure 2B). This positive rate was confirmed by multiple experiments (Figure 2C), which indicated that MSLN-CAR-T cells could specifically target MSLN. In addition, the expression of the CD3ζ from the CAR structure was significantly upregulated in MSLN-CAR-T cells compared to the negative control T cells 7 days after infection (Figure 2D). The size of endogenous CD3ζ in T cells is about 19 kD, and the predicted size of the recombinant MSLN-CAR protein was 72 kD, which is consistent with the western blot results (Figure 2D).

Characterization of lymphocytic phenotypes of MSLN-CAR-T cells

We determined the composition and phenotypes of $CD4^+$ and $CD8^+$ T cell subsets between the control T cells and MSLN-CAR-T cells by flow cytometry. Previous studies have shown that T cell differentiation can significantly impact the outcome of immunotherapy. Using surface CD45RA, CD62L, CCR7, and CD95 antigens, $CD4^+$ and $CD8^+$ T cells can be subdivided into T stem cell memory (Tscm; $CD45RA^+$ $CCR7^+CD62L^+CD95^+$), T effector memory (Tem; $CD45RA^-CCR7^-$), T central memory (Tcm; $CD45RA^-CCR7^+$), and T effector (Teff; $CD45RA^+CCR7^-$) cells. Tscm cells cause a more sustained anti-tumor effect compared to Tcm cells.[17] Our results indicated that $CD4^+$ and $CD8^+$ Tscm accounted for the highest proportion of T cells (Figure 3A).

When we evaluated checkpoint biomarkers, we found discrepancies between the lentivirus-infected and uninfected T cell samples; TIM3 and PD1 proteins significantly reduced (Figure 3B). Whether these changes could cause a positively regulated tumor immune response requires further investigation and is beyond the scope of this paper.

Evaluation of the anti-tumor capacity of MSLN-CAR-T cells *in vitro*

We selected ovarian (SKOV3, OVCAR3, ES2), gastric (AGS), intestinal (HCT116), breast (MCF7), and cervical (HeLa) cancer cell lines to evaluate the antitumor effects of MSLN-CAR-T cell *in vitro*. Flow cytometry confirmed that all cell lines, except ES2, were MSLN-positive (Figure 4A). To determine the cytotoxic activity, we co-cultured MSLN-CAR or control T cells with the above cell lines (effector [E]: target [T] = 2.5:1), and then assessed cytotoxicity by real-time cell analysis (RTCA) monitoring. The results showed that MSLN-CAR-T cells efficiently poisoned all MSLN-positive cell lines but not MSLN-negative ES2 cells. In contrast, the negetive control (NC)-T cells and the MSLN-CAR-T cells have a significant difference in cell killing ability (Figure 4B; Figure S1). Consistent with the RTCA data, significant amounts of interferon-γ (IFN-γ) and tumor necrosis factor alpha (TNF-α) were released into the medium 24 h after the co-culturing of the MSLN-CAR-T cells with the MSLN-positive cancer cell lines but not with ES2 cells (Figure 4C). In order to visually observe the killing effect of MSLN-CAR-T cells on target cells, we repeated the killing experiment on HCT116 in an ordinary 96-well plate, and representative bright-field images were shown in Figure 4D. The results clearly showed that the HCT116 cells in the CAR-T cell group were significantly reduced and the CAR-T cells clumped in the vicinity of the tumor cells.

Anti-tumor efficacy of MSLN-CAR-T cells against ovarian cancer *in vivo*

To determine the anti-tumor effect of MSLN-CAR-T cells against ovarian cancer, we used the SKOV3 CDX model (n = 4). This MSLN-positive ovarian cancer model was selected due to its rapid cell growth and short time for tumor establishment. A schematic of the experimental events and nodes for the *in vivo* model construction and treatment is presented in Figure 5A. During the 7 days after the injection, the tumor size of the two groups of mice showed an upward trend. However, starting from the 7th day, the tumors of the mice injected with MSLN-CAR-T cells began to weaken significantly until they completely subsided on the 17th day and the presence of tumors was not detected at all while tumors of mice treated with control T cells expanded rapidly (Figure 5B). We also observed that the mice in the control T cells-treated groups were in a state of malaise at the later stages of tumor development; however, the mice treated with MSLN-CAR-T cells remained in good condition and there was

Table 2. MSLN positivity rate in OC and OB samples

	Totals	High positive	Medium positive	Low positive	Negative	Positive rate (%)
OC	19	6	6	0	7	63.2
OB	13	0	0	2	11	15.3

OC, ovarian cancer tissue; OB, ovarian benign tissue

no significant difference in weight at the endpoint of the study between the two groups (Figure 5C).

Anti-tumor efficacy of MSLN-CAR-T cells against breast cancer *in vivo*

We also evaluated the efficacy of MSLN-CAR-T cells *in vivo* using the MCF7 breast cancer CDX model. 10 days after the cell inoculation, the mice were divided into the NC-T and MSLN-CAR-T groups (n = 3; Figure 6A). There were significant differences in tumor size between the MSLN-CAR-T and NC-T groups (Figure 6B). No significant difference was observed in body weight between the two experimental groups throughout the experiment (Figure 6C).

Anti-tumor efficacy of MSLN-CAR-T cells against colorectal cancer *in vivo*

The effect of MSLN-CAR-T cell therapy on colorectal tumors was examined using the HCT116 CDX model. 10 days after tumor cell inoculation, the mice were divided into three groups (n = 4) treated with PBS, NC-T cells, or MSLN-CAR-T cells (Figure 7A). 13 days after injection, the tumors of the MSLN-CAR-T group were significantly smaller than those of the other two groups. By day 24, the tumors in the PBS and NC-T groups reached the size endpoint of 1,500 mm^3, and the mice had to be euthanized. However, the tumors in the MSLN-CAR-T group remained small even at day 28 (Figure 7B). The mice in the CAR-T group were euthanized on day 28, and the tumors were compared to the other experimental groups. Differences in tumor size and weight were observed (Figures 7D and 7E). Throughout the experiment, there were no significant body weight changes among the three groups (Figure 7C). On day 20 (10 days after MSLN-CAR-T cell injection), peripheral blood was collected from the mice and analyzed for CD3. The CAR-T group had more $CD3^+$ T cells (Figure 7F). In contrast, the NC-T cells were only found in small frequency in the peripheral blood. We observed some differences in IFN-γ expression among the groups, but the differences did not reach statistical significance. These differences may be due to variations in IFN-γ expression in individual animals (Figure 7G). IHC on the tumor tissues taken from these mice showed that the MSLN-CAR-T group had higher GramB expression levels compared to the other groups (Figure 7H). Therefore, the MSLN-CAR-T cells had significant anti-tumor efficacy against a colorectal cancer CDX model.

Anti-tumor efficacy of MSLN-CAR-T cells against different PDX models *in vivo*

To confirm the effects, we observed with CDX models, we conducted MSLN-CAR-T cell therapy efficacy studies using gastric and colorectal cancer PDX mouse models (PDX-Gast0020 and PDX-col0092, respectively). The H&E staining and MSLN IHC results on the PDX tumors are shown in Figure 8A. The PDX-col0092 mice were randomly divided into MSLN-CAR-T (n = 5) and NC-T groups (n = 10) when the average tumor volume of each group was 25 mm^3. The two groups were injected with MSLN-CAR-T cells or NC-T, respectively. And when the tumors in the NC group grew to 1,000 mm^3, 5 mice were selected to be injected with MSLN-CAR-T to observe the pharmacological effects of MSLN-CAR-T on large-volume tumors (Figure 8B). Whether small or large tumor volume of the tumor, MSLN-CAR-T cells can show a good anti-tumor effect, and both the effective start time reflected on day 7 after injection. And in the drug efficacy experiment of large tumors, tumors with a maximum volume of 1,500 mm^3 can still be eliminated and finally stabilized at the very small tumor stage (Figure 8C). During the whole experiment, the weight of the mice did not change abnormally, but after 120 days of the experiment, one of the mice in the small tumor group was observed obvious xenogenic graft versus host disease (GvHD), which showed significant hair loss. But until the end of the experiment, the mice in the drug effect group did not die (Figures 8D and 8E). When the experiment reached the endpoint, we performed tumor genome quantitative PCR (qPCR) detection on three mice in the large tumor group that still had tumors, and the results showed that the tumors still had the MSLN-CAR genome (Figure 8F). For PDX-Gast0020, MSLN-CAR-T cells were injected only once (Figure 8G). The PDX-Gast0020 tumors rapidly progressed in the NC-T group. In contrast, MSLN-CAR-T cells demonstrated good anti-tumor efficacy against these colorectal cancer tumors (Figures 8H and 8I).

DISCUSSION

Despite the various treatments available for solid tumors (e.g., surgery, radiotherapy, chemotherapy, and targeted therapy), the prognosis for patients with solid tumors remains poor.[18,19] Therefore, more effective solid cancer therapies are still needed. The concept of CAR-T cell therapy was first mentioned in the 1980s; however, CAR-T technology did not demonstrate *in vivo* anti-tumor effects due to the structural limitations at the time.[20] In recent years, structure-modified and high-efficiency CAR-T cell therapy has been effective *in vivo*.[21,22] Two CAR-T cell products for acute ALL and advanced lymphoma have demonstrated the potential clinical application of this therapy. Moreover, the extraordinarily efficient CD19 CAR-T cell therapy against hematologic malignancies suggests the possibility of CAR-T cell therapies against solid tumors.[23,24]

To generate more effective CAR-T cells, it is crucial to select appropriate antigens to decrease tumor cells with minimum toxicity. An

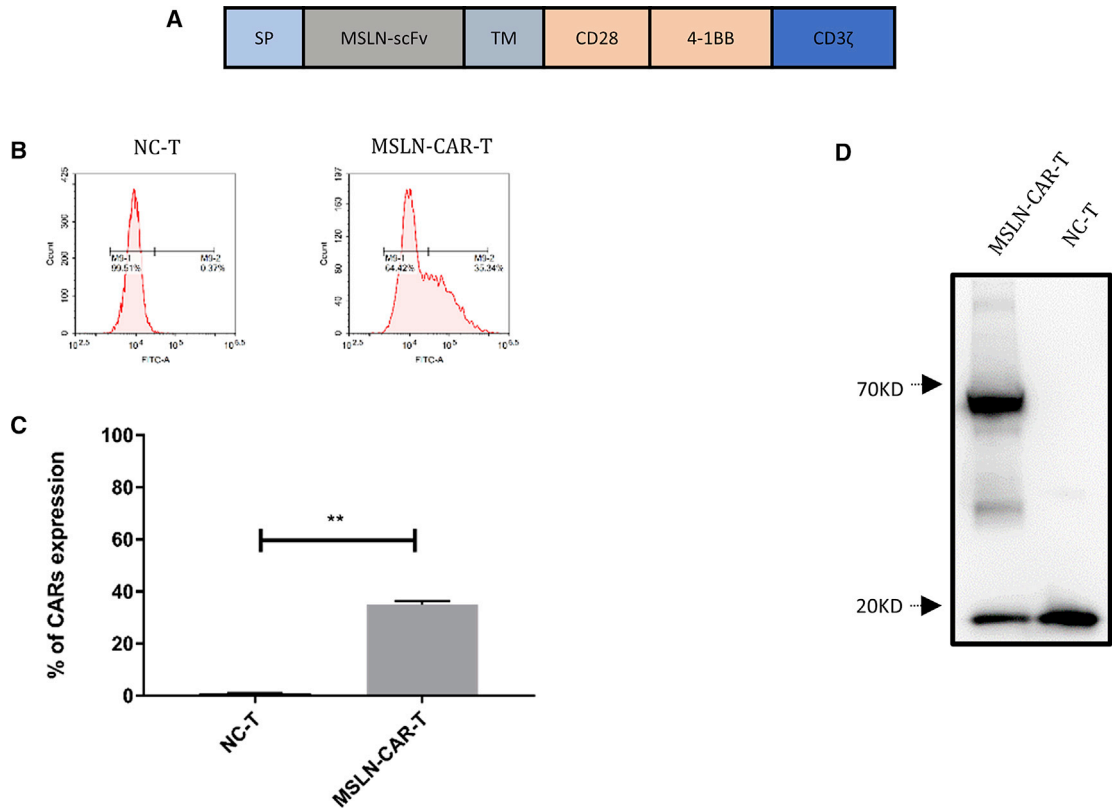

Figure 2. Characterization of 3rd-generation MSLN-CAR-T cells targeting MSLN

(A) Schematic diagram of the MSLN-CAR-T transgene. (B) Proportion of M284bz infected primary human T cells determined by flow cytometry. (C) Histogram of the MSLN-CAR-T rate of M28z10 CAR infected cells and its control cells in three repeats. (D) The exogenous CD3ζ level detected by western blotting (mean ± SEM; ns, not significant; $p > 0.05$, *$p < 0.05$, **$p < 0.01$, ***$p < 0.001$).

ideal solid tumor CAR-T-target should be significantly overexpressed in cancer cells but very lowly expressed or absent in non-vital normal tissue.[25] MSLN is a cell-surface antigen, which is highly expressed in a variety of cancers, including mesothelioma, lung, ovarian, and breast, but expressed at low levels in normal tissues.[8] We selected MSLN as the target for our third generation CAR structure because of its high expression in solid tumors, and we generated effective MSLN-CAR-T cells.

To date, there have been reports of CAR-T cell therapy targeting MSLN in solid tumors that not only demonstrated the effectiveness of this method but also established its safety.[10,11,26] Our study expanded the scope of MSLN targets to breast, ovarian, gastric, and colorectal cancer. Our approach still used a lentiviral plasmid as the gene delivery medium. There have been many reports describing non-viral vectors. Beatty et al.[10] used mRNA as the vector in a clinical phase 1 trial, demonstrating the validity of MSLN-CAR-T cell therapy. However, mRNA has a short half-life in cells, and its long-term sustained effect in the body is poor, which is reflected in the results. Other methods include electrotransformation of plasmids,[27] but there is no research to prove that the damage of cells caused by electrotransformation will not affect their subsequent functions. We first introduced the PDX model for evaluation of MSLN-CAR-T cell therapy. The PDX model preserves tumor heterogeneity and tissue structure, the aggressive vasculature, and supporting interstitial cells. Tumor cells grow in a transplanted environment, which provides the physiological oxygen concentration and nutritional environment of the tumor tissue in the body and provides a physiological substrate for tumor cell adhesion.[28,29] Compared with CDX models, the cytogenetic analysis of PDX models suggests that the PDX retains the chromosomal structure of the source tumor.[30] Our PDX model experiments showed that MSLN-CAR-T cell treatment had excellent anti-tumor activity (Figure 8).

We encountered some problems during our study. When we selected the animal models, the initial tumor size was maintained at the level of 50 mm^3, so that the final effect would be particularly obvious. Carpenito et al.[31] showed that tumors could regress when treated at a size of 500 $mm.^3$ A larger tumor indicates a more severe tissue suppression and complex tumor microenvironment, which greatly reduces T cell infiltration into the tumor.[32,33] After constantly trying different mouse models, we found PDX-COL0092, an experimental case that can eliminate large tumors (1,000 mm^3 on average). Even when the tumor grows to 1,000 mm^3, the same amount of MSLN-CAR-T

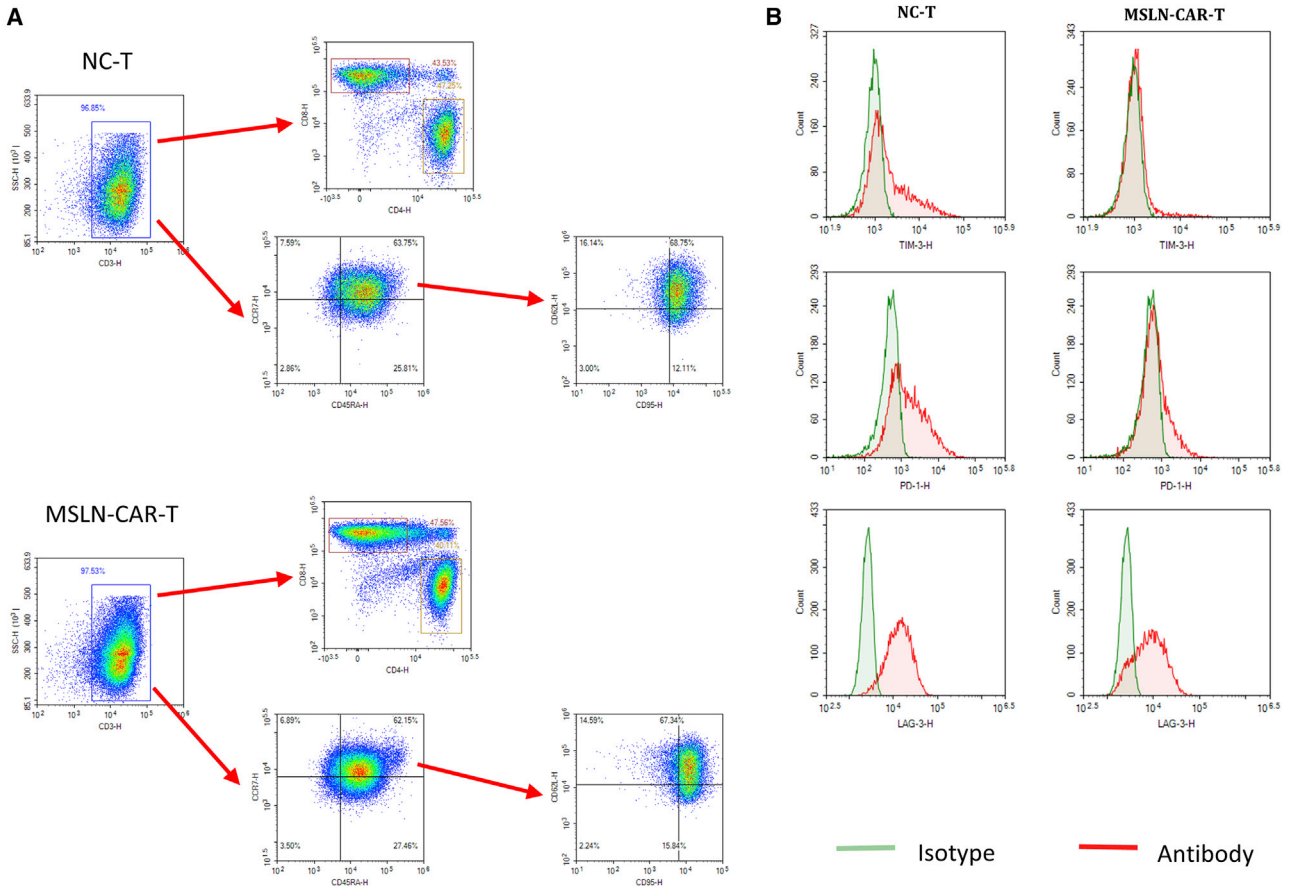

Figure 3. Phenotype and changes of MSLN-CAR-T cells

(A) Flow cytometry to detect $CD3^+/CD4^+/CD8^+/CD45RA^+/CCR7^+/CD62L^+/CD95^+$ ratio in CAR-T cells and NC-T cells (B) Detection exhaustion biomarker of TIM3, PD1, and LAG3 on CAR-T cells and NC-T cells by flow cytometry.

(2.5×10^6 CAR^+ cells) was injected with the small tumor (50 mm^3 on average), and obvious tumor regression can still be seen (Figure 8). It showed that the tumor tissue of this model may be different from other tumor tissues, and this difference may be the key to CAR-T cell treatment of large tumors. Given the effects of the microenvironment on T cells, several optimized combination treatment strategies have emerged, including co-expression of cytokines to help enhance autoimmunity and co-expression of checkpoint protein antibodies (e.g., PD1 and PDL1 antibodies) that could suppress the side effects mediated by the immune checkpoint pathways.[34] In the future, we will further optimize the CAR structure to enhance the CAR-T cell anti-tumor effect.

In summary, our results confirmed that our third generation MSLN-CAR-T cells killed not only specific MSLN-positive cancer cells *in vitro*, but also MSLN-positive CDX and PDX solid tumors *in vivo*. Our results against a diverse panel of tumors suggest that MSLN-CAR-T cells could represent a potential breakthrough in the treatment of solid tumors. More clinical trials should be initiated to evaluate MSLN-CAR-T cell therapy for the treatment of MSLN-positive solid tumors.

MATERIALS AND METHODS

Construction of CAR vector

The third generation MSLN-CAR contains the MSLN-specific target scFv with a CD8 leading sequence, a CD8 hinge and transmembrane sequence, and the intracellular signaling domain of 4-1BB, CD28, and CD3ζ in tandem. The full-length nucleotide sequence was synthesized (Shenggong, Shanghai, China) and inserted into lentiviral vector pCDH-CMV-MCS-EF1-puro using the BstbI and NotI cloning sites.

Lentivirus packaging and production

Viruses were collected from the supernatants of HEK293T cells transfected with the MSLN-CAR lentivirus vector and two helper packaging plasmids (psPAX2 and pMD.2G) using polyethyleneimine (Polyscience, Warrington, PA, USA). Lentivirus-rich supernatants were collected 24 h, 48 h, and 72 h post-transfection and filtered through a 0.45-μm filter.

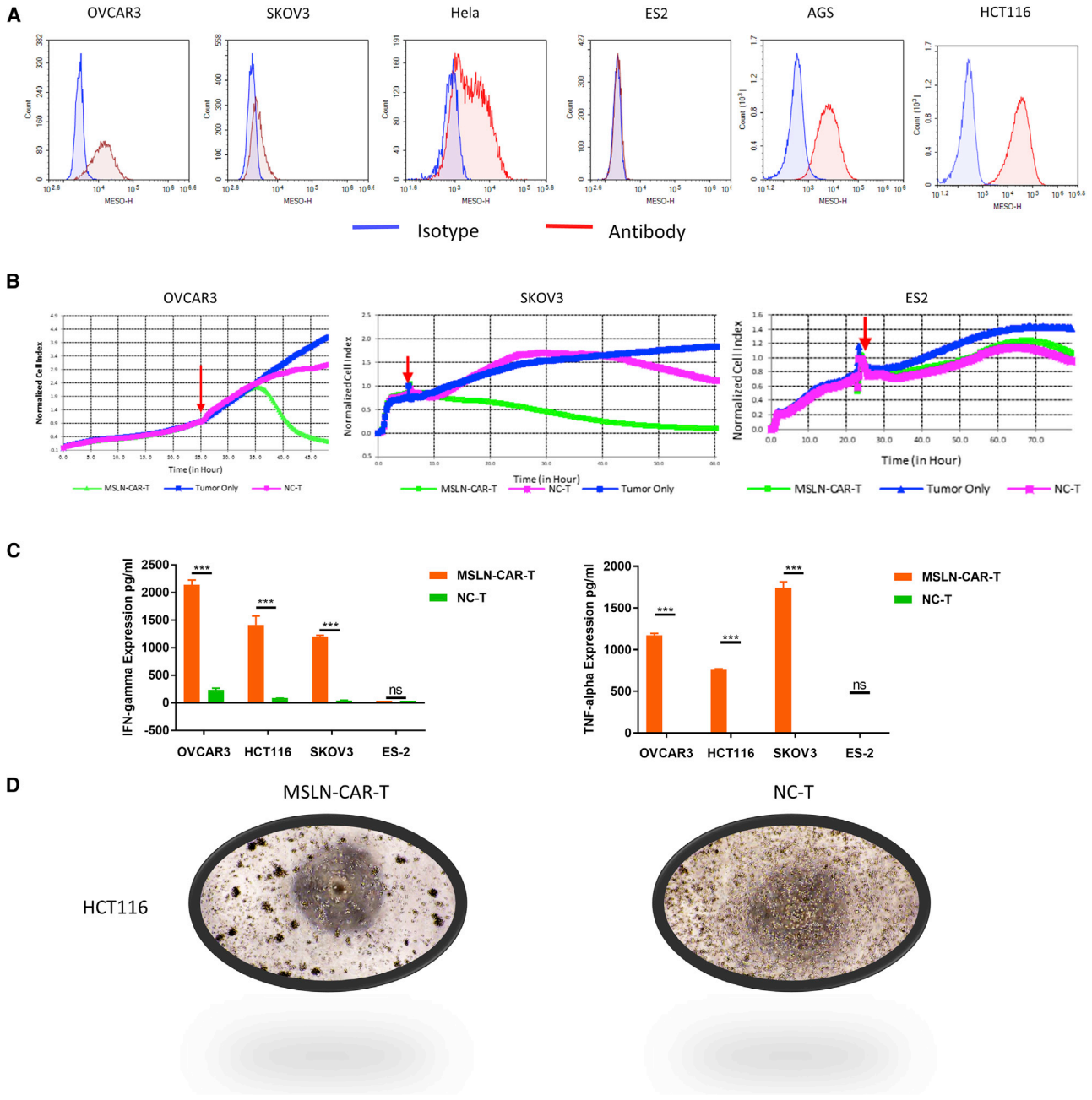

Figure 4. Evaluation of the anti-tumor capacity of MSLN-CAR-T cells *in vitro*

(A) The surface expression of MSLN receptor level on solid tumor cell lines (OVCAR3, SKOV3, HeLa, ES2, AGS, HCT116) detected by flow cytometry. (B) The cytotoxicity of MSLN-CAR-T cells against solid tumor cell lines was analyzed by RTCA assay. The red arrow represents the time point of effector cell addition. (C) Levels of IFN-γ and TNF-α released by MSLN-CAR-T cells analyzed by ELISA after incubated with cells for 24 h. (D) A549 and HeLa weren't shown, mean ± SEM; $p > 0.05$, $^{*}p < 0.05$, $^{**}p < 0.01$, $^{***}p < 0.001$).

Isolation of primary PBMCs and transduction of T cells

Fresh blood was collected from healthy volunteers after informed consent under a protocol approved by the Ethics Committee of Nantong Tumor Hospital. Peripheral blood mononuclear cells (PBMCs) were isolated from normal donor blood buffy coats using Ficoll (GE). T cells were separated from PBMCs using SepMate mononuclear cell isolation tubes (STEMCELL Technologies, Vancouver, BC, Canada). Primary cells were cultured in T cell medium containing GT-T551H3 (Takara, Kyoto, Japan) and 1% penicillin-streptomycin-glutamine (Gibco, Gaithersburg, MD, USA). MSLN-CAR-T cells were generated by lentiviral transduction of normal donor T cells. Briefly, T cells were isolated from normal donors and

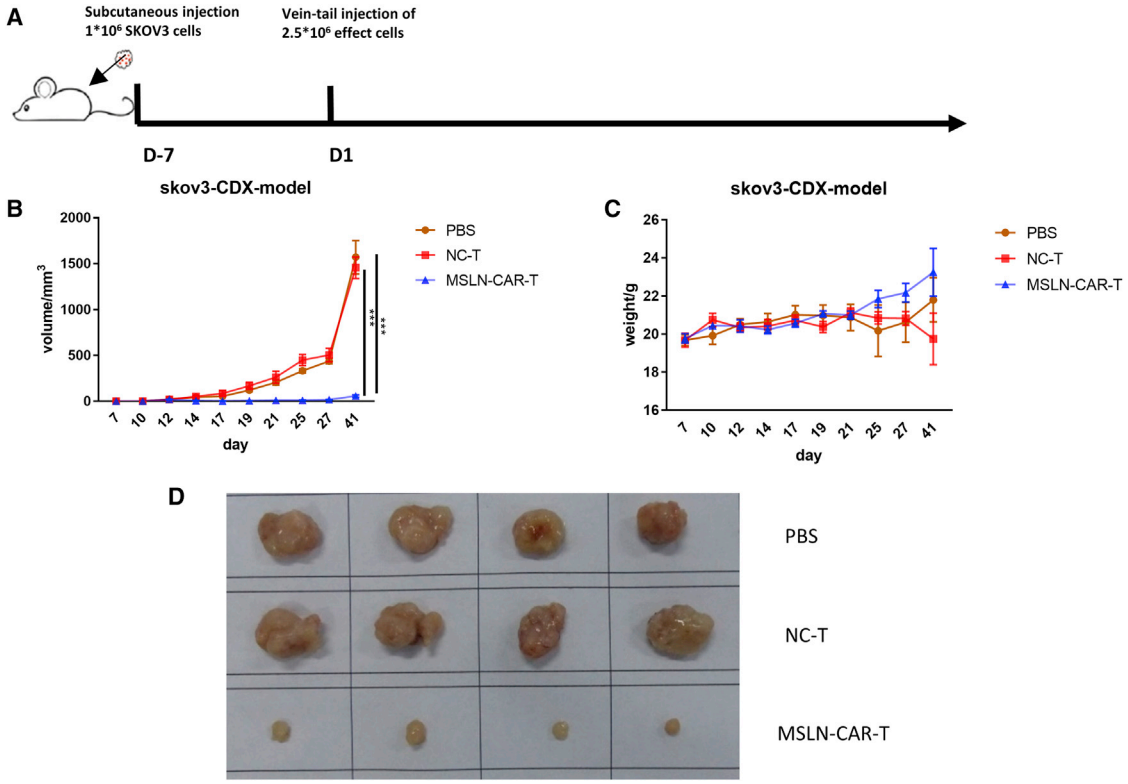

Figure 5. Anti-tumor efficacy of MSLN-CAR-T cells against ovarian cancer *in vivo*

(A) Schema of the experimental events and nodes. In this process, model mice were injected with 1 × 10^6 OC cells SKOV3. 7 days after injection, 8 mice were randomly divided into 2 groups (n = 4): 2.5 × 10^6 MSLN-CAR-T cells-treated group and control-T cells-treated group. (B and C) The tumor size (B) and mice weight (C) variation with MSLN-CAR-T cells, control T cells, or PBS injection among the 35 days.(D) Size of SKOV3 CDX tumor mass differed in MSLN-CAR-T cells, control T cells or PBS treated mice. (n = 4, mean ± SEM; $p > 0.05$, *$p < 0.05$, **$p < 0.01$, ***$p < 0.001$).

then activated using microbeads coated with anti-human CD3 and CD28 antibodies (CytoCares, Shanghai, China) at a 1:1 bead to cell ratio. The T cells were infected with lentivirus 24 h post-stimulation at a multiplicity of infection of 30. After infection, the T cells were cultured in fresh medium containing interleukin-2 (IL-2; 150 IU/mL), with the medium replaced every 2–3 days.

Western blot analysis

To confirm CAR expression in the transduced T cells, we denatured cell lysates, separated them by SDS-PAGE, and transferred them to nitrocellulose membranes (Bio-Rad, Hercules, CA, USA). After blocking, the membranes were incubated with an anti-CD3ζ primary antibody (CD247, BD, USA), followed by incubation with horseradish peroxidase (HRP)-conjugated secondary antibodies. Protein bands were exposed to enhanced chemiluminescence (ECL; GE, Healthcare, USA) and detected by autoradiography. Untransduced T cells were used as controls.

Cells and culture conditions

HEK293T, human ovarian cancer cell lines (SKOV3, OVCAR3, ES2), human cervical carcinoma cell line HeLa, human breast cell line MCF7, human gastric adenocarcinoma cell line AGS, and human colorectal cancer cell line HCT116 were obtained from the Cell Bank of the Chinese Academy of Sciences (Shanghai, China). SKOV3 and ES2 were maintained in McCoy's 5A medium (Gibco, Grand Island, NY, USA). OVCAR3 was maintained in RPMI-1640 medium (Gibco, Grand Island, NY, USA). HEK293T, MCF7, and HCT116 were maintained in Dulbecco's modified Eagle's medium (DMEM, Gibco, Grand Island, NY, USA), and AGS was maintained in F12 medium (Gibco, Grand Island, NY, USA), HeLa was maintained in MEM (Gibco, Grand Island, NY, USA). All complete cell culture medium contained 10% heat-inactivated FBS (Gibco/Life Technologies, Shanghai, China), 10 mM HEPES, 2 mM glutamine (Gibco/Life Technologies, Shanghai, China), and 1% penicillin/streptomycin (Gibco/Life Technologies, Shanghai, China). All cells were cultured at 37°C in an atmosphere of 5% CO_2.

Flow cytometry

Flow cytometry cell staining was performed at 4°C in PBS supplemented with 2% FBS, unless otherwise indicated. The expression of MSLN on cancer cells was detected by flow cytometry, using a human MSLN PE-conjugated antibody (R&D, FAB32652P, USA).

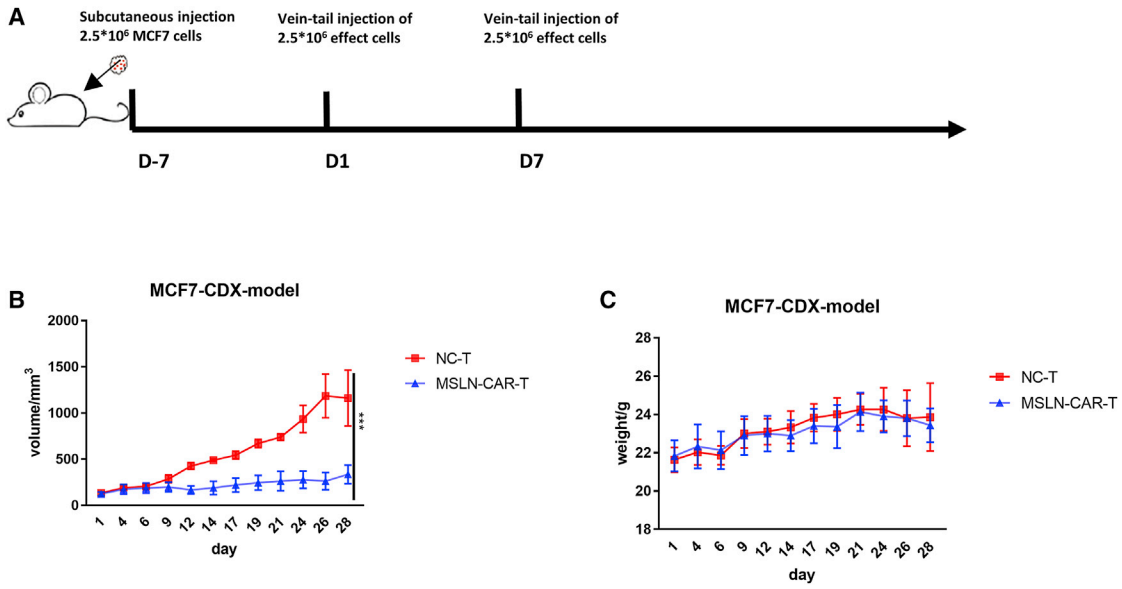

Figure 6. Anti-tumor efficacy of MSLN-CAR-T cells against breast cancer *in vivo*

(A) Schema of the experimental events and nodes. In this process, model mice were injected with 2.5×10^6 breast cancer cell MFC7. 27 days after injection, 6 mice were randomly divided into 2 groups (n = 3): 2.5×10^6 MSLN-CAR-T cells-treated group and control-T cells-treated group. Injections were given every week, for a total of two times. (B and C) The tumor size (B) and mice weight (C) variation with MSLN-CAR-T cells, control T cells or PBS injection among the 41 days (n = 3, mean ± SEM; $p > 0.05$, $^*p < 0.05$, $^{**}p < 0.01$, $^{***}p < 0.001$).

The expression of CAR on CAR-T cells was detected using biotinylated human MSLN (Acro, Beijing, China), followed by staining with allophycocyanin (APC) streptavidin (BioLegend, CA, USA).

The immunophenotypes of T cells were tested using flow cytometry. The antibodies used for analysis include: APC-Cy 7 mouse anti-human CD3 (BD, NJ, USA), APC mouse anti-human CD4 (BD, NJ, USA), phycoerythrin (PE) mouse anti-human CD8 (BD, Franklin Lakes, NJ, USA), Brilliant Violet 421 anti-human CD197 (BioLegend, CA, USA), fluorescein isothiocyanate (FITC) anti-human CD45RA (BioLegend, San Diego, CA, US), PE-Cy7 anti-human CD45RO (BioLegend, San Diego, CA, USA), Brilliant Violet 421 anti-human CD197 (CCR7; BioLegend, San Diego, CA, USA), Brilliant Violet 510 anti-human CD62L (BioLegend, San Diego, CA, USA), Brilliant Violet 605 anti-human CD95 (Fas; BioLegend, San Diego, CA, USA), PE anti-human CD223 (LAG-3; BioLegend, San Diego, CA, USA), Brilliant Violet 421 anti-human CD366 (Tim-3; BioLegend, San Diego, CA, USA), and APC anti-human CD279 (PD-1; BioLegend, San Diego, CA, USA). Data were analyzed using NovaExpr software (ACEA, Ashland, OR, USA).

In vitro cytotoxicity assays

Tumor cells were seeded in 96-well E-plates (ACEA Biosciences, Menlo Park, CA, USA). After 20 h, control or MSLN-CAR-T cells were added to the plates at a target ratio of 2.5:1. Untransduced T cells were used as NC-T and added to the control group. The group that did not add the effector cells was called tumor-only group. The viability of the target cells was detected using the RTCA system (xCElligence RTCA SP, ACEA, Los Angeles, CA, USA) according to the manufacturer's protocol. The cell index was recorded every 15 min.

Cytokine release assays

Cytokine release assays were carried out using a human IFN-γ (88-7316-88, eBioscience, Thermo Fisher Scientific, Shanghai, China) and TNF-α (88-7346-88, eBioscience) ELISA kits. MSLN-CAR-T cells were co-cultured with target cells at a ratio of 2.5:1. After 24 h, the supernatant was collected, and the IFN-γ and TNF-α levels were measured according to the manufacturer's instructions.

Mouse tumor models for MSLN-CAR-T cell treatment

All animal experiments were carried out in the Shanghai Beautiful Life Animal Center, and all animal procedures and protocols were approved by the Animal Welfare Committee of Shanghai Beautiful Life Animal Center. All mice were maintained in specific pathogen-free (SPF) cages and provided clean food and water. NOD-Prkdcem26IL2rgem26/Nju (NCG) mice were purchased from NBRI (Nanjing, China). For the CDX models, SKOV3 (1.0×10^6), HCT116 (5.0×10^5), or MCF7 (2.5×10^6) cells were injected subcutaneously into 6- to 8-week-old NCG mice in a volume of 100 μL PBS. When tumors were palpable, the mice were divided into three groups. An equal number of MSLN-CAR-T or untransduced T cells were injected into the mice of the CAR-T and NC-T control groups, respectively. Each MSLN-CAR-T cell injection contained 2.5×10^6 CAR-positive cells. The total cell number was calculated from the positive rate. The untransduced T cells were injected according to the calculated total cell number. When any of the following occurred,

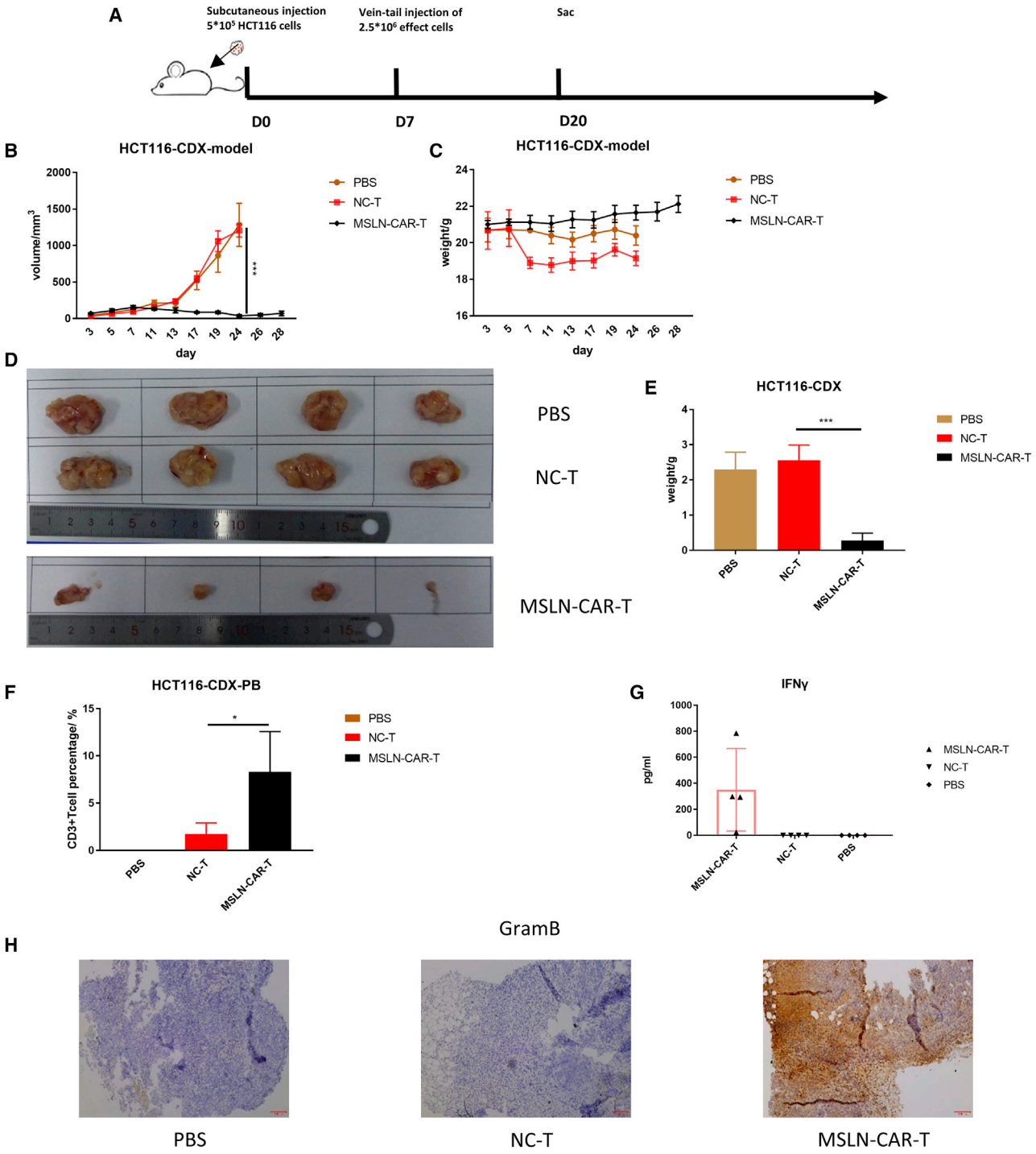

Figure 7. Anti-tumor efficacy of MSLN-CAR -T cells against colorectal cancer *in vivo*

(A) Schema of the experimental events and nodes. In this process, model mice were injected with 5×10^5 CRC cells HCT116. 10 days after injection, 12 mice were randomly divided into 3 groups (n = 4): 5×10^6 MSLN-CAR-T cells-treated group, control-T cells-treated group, and PBS of the same volume-treated group. After only one injection, we started observing the mice. (B and C) The tumor size (B) and mice weight (C) variated with MSLN-CAR-T cells, control T cells, or PBS injection among the 28 days. (D) Size of tumor mass differed in MSLN-CAR-T cells, control T cells, or PBS-treated mice. (E) Weight of tumor mass differed in MSLN-CAR-T cells, control T cells, or PBS-treated mice. On day 20, the mice were sacrificed; the $CD3^+$ T cell amount in the PB of HCT116 CDX model is as shown (F). The level of IFN-γ in mouse serum was evaluated by ELISA as shown (G). (H) Immunohistochemistry (IHC) analysis of granzyme B in tumor sections (n = 4, mean ± SEM; $p > 0.05$, $^*p < 0.05$, $^{**}p < 0.01$, $^{***}p < 0.001$).

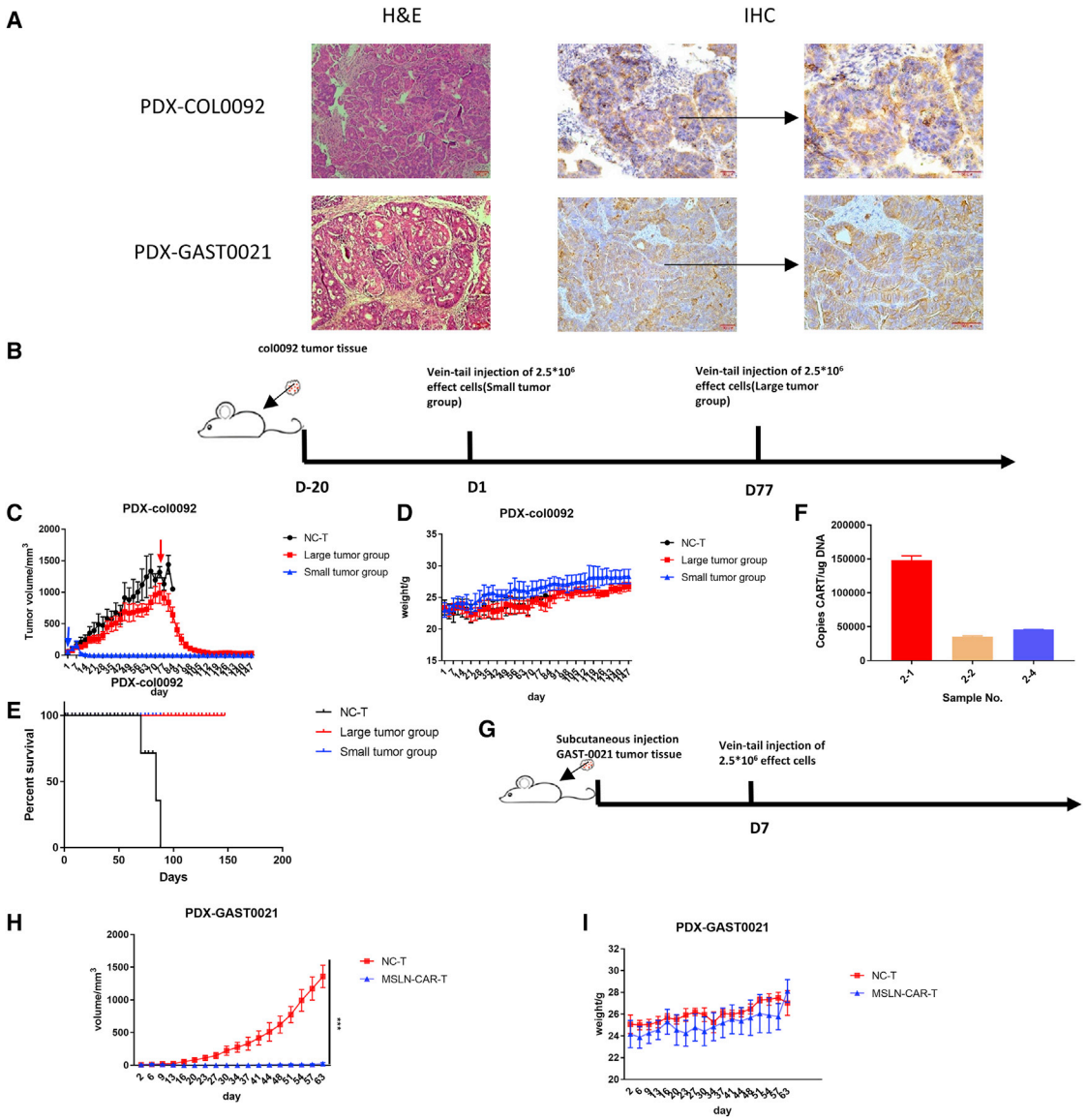

Figure 8. Anti-tumor efficacy of MSLN-CAR-T cells against different PDX models *in vivo*

(A) The result of hematoxylin and eosin (H&E) and antibody against MSLN. (B and G) Schema of the experimental events and nodes. After the establishment of the PDX model, the mice were randomly divided into two groups (PDX-COL0092 n = 5, PDX-GAST0021 n = 4), CAR-T group and NC-T group. (C, D, H, and I) The tumor size (C and H) and mice weight (D and I) variated with MSLN-CAR-T cells and control T cells injection during the observed time. (E) Kaplan-Meier curves for survival of the PDX-COL0092 models are shown. (F) At the end of the experiment in the PDX-COL0092 group, the MSLN-CAR gene copies in the tumor in the experimental group that still had the tumor were detected by qPCR, and representative results from one of three experiments are shown (mean ± SEM; $p > 0.05$, $^{*}p < 0.05$, $^{**}p < 0.01$, $^{***}p < 0.001$).

the experiment was stopped immediately and the mice were euthanized: the size of the tumor exceeded 2,000 mm3, the weight of the mouse decreased by more than 25%, and the mice could not eat for more than 48 h. The tumor ulcerated or caused significant pain. The tumor affected the normal movement and behavior of the mice. Tumor size was measured twice per week with a caliper, and the tumor volume was calculated by the following equation: volume = (length × width2)/2, where length represents the longest dimension.

For the PDX models, surgical colorectal and gastric tumor samples were obtained from the Nantong Tumor Hospital (Nantong, China) with informed consent from the patients. All patients who provided primary specimens gave informed consent to use the samples for research purposes. All procedures were approved by the Research Ethics Board of Nantong Tumor Hospital. The tumors were cut into 2 mm × 2 mm pieces and directly transplanted subcutaneously into 2 to 4 immunodeficient NCG mice within a 30-min period.

Tumors that reached an approximate size of <1,000 mm^3 were removed and passaged into additional NCG mice. For the CAR-T experiments, when the size of the inoculated tumors reached 20 to 50 mm^3, the mice were divided into the CAR-T efficacy and NC-T control groups. The colorectal and gastric cancer PDX models were treated with MSLN-CAR-T cells or NC-T, as described for the CDX models.

IHC

Ovarian tumor and benign tissues were obtained from the First Affiliated Hospital of Dalian Medical University (Dalian, China), and colorectal tumor tissue was obtained from Nantong Tumor Hospital (Nantong, China). All tumor and benign tissue samples were acquired with informed consent from the patients. All patients who provided primary specimens gave informed consent to use the samples for research purposes. All procedures were approved by the Research Ethics Board of the First Affiliated Hospital of Dalian Medical University and Nantong Tumor Hospital. The tumor samples that appeared during the experiment were the tumor tissues confirmed by the pathology department of the hospital, the non-tumor tissue samples of the colorectal were paracancerous tissue samples, and the non-tumor tissue samples of the ovary were benign tumors or cysts confirmed by the pathology department. The tissues were fixed with 10% paraformaldehyde, embedded in paraffin, sectioned at a thickness of 4 μm, and immunostained with a MSLN-specific antibody (99966S, CST, USA) overnight at 4°C, followed by secondary staining with secondary goat anti-rabbit immunoglobulin (Ig; PV-9000; ZSGB-BIO, Beijing, China). Images of the stained sections were captured with an Olympus BX53 microscope (Japan).

qPCR analysis to detect MSLN-CAR copies

Total genomic DNA was isolated directly from tumor tissue by DNeasy Blood & Tissue Kit (QIAGEN, 69506). qPCR reactions were performed in triplicate with Taqman prob premix (TAKARA). The relative quantification of the products was calculated by the $2^{-\Delta\Delta Ct}$ method. The following specific primers were synthesized and obtained from Sunnybio (Shanghai, China):

MSLN-CAR (forward), 5′-CTCTCTCGACGCAGGACTC-3′; MSLN-CAR (reverse), 5′-TCTAGCCTCCGCTAGTCAAA-3′; MSLN-CAR (probe), 5′-CGGCGACTGGTGAGTACGCCAA-3′.

Statistical analysis

Statistical analysis was performed using GraphPad Prism 5.0 (GraphPad Software, San Diego, CA, USA). All experiments were repeated at least three times. The Student's t test was used to compare the two groups. p value <0.05 indicated statistical significance (*$p < 0.05$, **$p < 0.01$, and ***$p < 0.001$).

SUPPLEMENTAL INFORMATION

Supplemental Information can be found online at https://doi.org/10.1016/j.omto.2021.02.013.

ACKNOWLEDGMENTS

This research was supported by Shanghai Science and Technology Committee (STCSM; grant numbers 19ZR1454700 and 202H1020600).

AUTHOR CONTRIBUTIONS

X.T., Q.Z., and Lixin Zhang designed the study, performed data analysis, and wrote the manuscript. G.L., J.L., and J.F. participated in sample collection and animal experiments. M.Y., G.L., D.L., Linsong Zhang, L.W., and Z.G. performed some experiments. M.Y., Linsong Zhang, Y.P., and X.C. participated in critical revision of the manuscript. The current manuscript has been read and approved by all named authors.

DECLARATION OF INTERESTS

The authors declare no competing interests.

REFERENCES

1. The, L.; The Lancet (2018). GLOBOCAN 2018: counting the toll of cancer. Lancet *392*, 985.
2. Bray, F., Ferlay, J., Soerjomataram, I., Siegel, R.L., Torre, L.A., and Jemal, A. (2018). Global cancer statistics 2018: GLOBOCAN estimates of incidence and mortality worldwide for 36 cancers in 185 countries. CA Cancer J. Clin. *68*, 394–424.
3. Kruger, S., Ilmer, M., Kobold, S., Cadilha, B.L., Endres, S., Ormanns, S., Schuebbe, G., Renz, B.W., D'Haese, J.G., Schloesser, H., et al. (2019). Advances in cancer immunotherapy 2019 - latest trends. J. Exp. Clin. Cancer Res. *38*, 268.
4. Yong, C.S.M., Dardalhon, V., Devaud, C., Taylor, N., Darcy, P.K., and Kershaw, M.H. (2017). CAR T-cell therapy of solid tumors. Immunol. Cell Biol. *95*, 356–363.
5. Mardiana, S., Solomon, B.J., Darcy, P.K., and Beavis, P.A. (2019). Supercharging adoptive T cell therapy to overcome solid tumor–induced immunosuppression. Immunotherapy *11*, eaaw2293.
6. Gilham, D.E., Debets, R., Pule, M., Hawkins, R.E., and Abken, H. (2012). CAR-T cells and solid tumors: tuning T cells to challenge an inveterate foe. Trends Mol. Med. *18*, 377–384.
7. Chang, K., and Pastan, I. (1996). Molecular cloning of mesothelin, a differentiation antigen present on mesothelium, mesotheliomas, and ovarian cancers. Cell Biol. *93*, 136–140.
8. Zhang, Z., Jiang, D., Yang, H., He, Z., Liu, X., Qin, W., Li, L., Wang, C., Li, Y., Li, H., et al. (2019). Modified CAR T cells targeting membrane-proximal epitope of mesothelin enhances the antitumor function against large solid tumor. Cell Death Dis. *10*, 476.
9. Morello, A., Sadelain, M., and Adusumilli, P.S. (2016). Mesothelin-Targeted CARs: Driving T Cells to Solid Tumors. Cancer Discov. *6*, 133–146.
10. Beatty, G.L., O'Hara, M.H., Lacey, S.F., Torigian, D.A., Nazimuddin, F., Chen, F., Kulikovskaya, I.M., Soulen, M.C., McGarvey, M., Nelson, A.M., et al. (2018). Activity of Mesothelin-Specific Chimeric Antigen Receptor T Cells Against Pancreatic Carcinoma Metastases in a Phase 1 Trial. Gastroenterology *155*, 29–32.
11. Lv, J., Zhao, R., Wu, D., Zheng, D., Wu, Z., Shi, J., Wei, X., Wu, Q., Long, Y., Lin, S., et al. (2019). Mesothelin is a target of chimeric antigen receptor T cells for treating gastric cancer. J. Hematol. Oncol. *12*, 18.
12. Hiroshima, Y., Zhang, Y., Zhang, N., Maawy, A., Mii, S., Yamamoto, M., Uehara, F., Miwa, S., Yano, S., Murakami, T., et al. (2015). Establishment of a patient-derived orthotopic Xenograft (PDOX) model of HER-2-positive cervical cancer expressing the clinical metastatic pattern. PLoS ONE *10*, e0117417.
13. Kawaguchi, T., Foster, B.A., Young, J., and Takabe, K. (2017). Current Update of Patient-Derived Xenograft Model for Translational Breast Cancer Research. J. Mammary Gland Biol. Neoplasia *22*, 131–139.

14. Lai, Y., Wei, X., Lin, S., Qin, L., Cheng, L., and Li, P. (2017). Current status and perspectives of patient-derived xenograft models in cancer research. J. Hematol. Oncol. *10*, 106.

15. Ricci, F., Bizzaro, F., Cesca, M., Guffanti, F., Ganzinelli, M., Decio, A., Ghilardi, C., Perego, P., Fruscio, R., Buda, A., et al. (2014). Patient-derived ovarian tumor xenografts recapitulate human clinicopathology and genetic alterations. Cancer Res. *74*, 6980–6990.

16. MacKay, M., Afshinnekoo, E., Rub, J., Hassan, C., Khunte, M., Baskaran, N., Owens, B., Liu, L., Roboz, G.J., Guzman, M.L., et al. (2020). The therapeutic landscape for cells engineered with chimeric antigen receptors. Nat. Biotechnol. *38*, 233–244.

17. Biasco, L., Scala, S., Basso Ricci, L., Dionisio, F., Baricordi, C., Calabria, A., Giannelli, S., Cieri, N., Barzaghi, F., Pajno, R., et al. (2015). In vivo tracking of T cells in humans unveils decade-long survival and activity of genetically modified T memory stem cells. Sci. Transl. Med. *7*, 273ra13.

18. Wang, R.F., and Wang, H.Y. (2017). Immune targets and neoantigens for cancer immunotherapy and precision medicine. Cell Res. *27*, 11–37.

19. Abken, H. (2017). Driving CARs on the Highway to Solid Cancer: Some Considerations on the Adoptive Therapy with CAR T Cells. Hum. Gene Ther. *28*, 1047–1060.

20. Gross, G., Waks, T., and Eshhar, Z. (1989). Expression of immunoglobulin-T-cell receptor chimeric molecules as functional receptors with antibody-type specificity. Proc. Natl. Acad. Sci. *86*, 10024–10028.

21. Zah, E., Lin, M.Y., Silva-Benedict, A., Jensen, M.C., and Chen, Y.Y. (2016). T Cells Expressing CD19/CD20 Bispecific Chimeric Antigen Receptors Prevent Antigen Escape by Malignant B Cells. Cancer Immunol. Res. *4*, 498–508.

22. Heczey, A., Louis, C.U., Savoldo, B., Dakhova, O., Durett, A., Grilley, B., Liu, H., Wu, M.F., Mei, Z., Gee, A., et al. (2017). CAR T Cells Administered in Combination with Lymphodepletion and PD-1 Inhibition to Patients with Neuroblastoma. Mol. Ther. *25*, 2214–2224.

23. Wang, Z., Guo, Y., and Han, W. (2017). Current status and perspectives of chimeric antigen receptor modified T cells for cancer treatment. Protein Cell *8*, 896–925.

24. Zou, Y., Xu, W., and Li, J. (2018). Chimeric antigen receptor-modified T cell therapy in chronic lymphocytic leukemia. J. Hematol. Oncol. *11*, 130.

25. Oberaigner, W., Minicozzi, P., Bielska-Lasota, M., Allemani, C., de Angelis, R., Mangone, L., Sant, M., and Eurocare Working, G.; Eurocare Working Group (2012). Survival for ovarian cancer in Europe: the across-country variation did not shrink in the past decade. Acta Oncol. *51*, 441–453.

26. Zhao, R., Cheng, L., Jiang, Z., Wei, X., Li, B., Wu, Q., Wang, S., Lin, S., Long, Y., Zhang, X., et al. (2018). DNAX-activating protein 10 co-stimulation enhances the anti-tumor efficacy of chimeric antigen receptor T cells. OncoImmunology *8*, e1509173.

27. Li, H., Huang, Y., Jiang, D.Q., Cui, L.Z., He, Z., Wang, C., Zhang, Z.W., Zhu, H.L., Ding, Y.M., Li, L.F., et al. (2018). Antitumor activity of EGFR-specific CAR T cells against non-small-cell lung cancer cells in vitro and in mice. Cell Death Dis. *9*, 177.

28. Chijiwa, T., Kawai, K., Noguchi, A., Sato, H., Hayashi, A., Cho, H., Shiozawa, M., Kishida, T., Morinaga, S., Yokose, T., et al. (2015). Establishment of patient-derived cancer xenografts in immunodeficient NOG mice. Int. J. Oncol. *47*, 61–70.

29. Jung, J., Seol, H.S., and Chang, S. (2018). The Generation and Application of Patient-Derived Xenograft Model for Cancer Research. Cancer Res. Treat. *50*, 1–10.

30. Colombo, P.E., du Manoir, S., Orsett, B., Bras-Gonçalves, R., Lambros, M.B., MacKay, A., Nguyen, T.T., Boissière, F., Pourquier, D., Bibeau, F., et al. (2015). Ovarian carcinoma patient derived xenografts reproduce their tumor of origin and preserve an oligoclonal structure. Oncotarget *6*, 28327–28340.

31. Carpenito, C., Milone, M.C., Hassan, R., Simonet, J.C., Lakhal, M., Suhoski, M.M., Varela-Rohena, A., Haines, K.M., Heitjan, D.F., Albelda, S.M., et al. (2008). Control of large, established tumor xenografts with genetically retargeted human T cells containing CD28 and CD137 domains. Proc. Natl. Acad. Sci. *106*, 3360–3365.

32. Abken, H. (2015). Adoptive therapy with CAR redirected T cells: the challenges in targeting solid tumors. Immunotherapy *7*, 535–544.

33. Kakarla, S., and Gottschalk, S. (2014). CAR T Cells for Solid Tumors Armed and Ready to Go? Cancer J *20*, 151–155.

34. Khalil, D.N., Smith, E.L., Brentjens, R.J., and Wolchok, J.D. (2016). The future of cancer treatment: immunomodulation, CARs and combination immunotherapy. Nat. Rev. Clin. Oncol. *13*, 273–290.